Experimental investigations of boundary layer suction in a large index refraction channel

by

S. Becker

Institute of Fluid Mechanics (LSTM)

University Erlangen-Nuremberg

Cauerstr. 4

91058 Erlangen, Germany

E-Mail: sbecker@lstm.uni-erlangen.de

ABSTRACT

For the maintenance of the laminar boundary-layer flow on transonic wings, it is necessary to integrate a boundary layer suction unit in the nose-area. This concept of the Hybrid Laminar Flow control is realized through a suction area adapted at the outer pressure-distribution through suction holes array, with which a stabilization of the border-layer is reached opposite cross flow instabilities. Goal of the planned experimental examinations was to be widen the understanding of the until now achieved results of flow topology at a single hole suction on hole-array. Of particular interest was the influence of the hole-size, the hole-spacing and the suction flow rate (sub critical, critical and overcritical) on the receptivity of the boundary layer.

The work is conducted in the big refractive index canal of the LSTM, with which LDA - velocity-measurements closed to wall in the border-layer are possible. The Direct Numerical Simulations from the literature formed the basis of the chosen experimental parameters. The investigations were carried out by "free transition" conditions, i.e. it received no additional artificially, disturbance generated brought in before the suction holes row into the boundary layer. In the examinations, the physical mechanisms of the transition acceleration as well as -deceleration could be clarified in dependence of the suction rate. In contrast to the direct numerical simulations of the transition process with the increase of Tollmien-Schlichting-waves propagation (linear stability-theory) is described. From the achieved results it is shown that the transition process possesses a strong stochastic behavior.

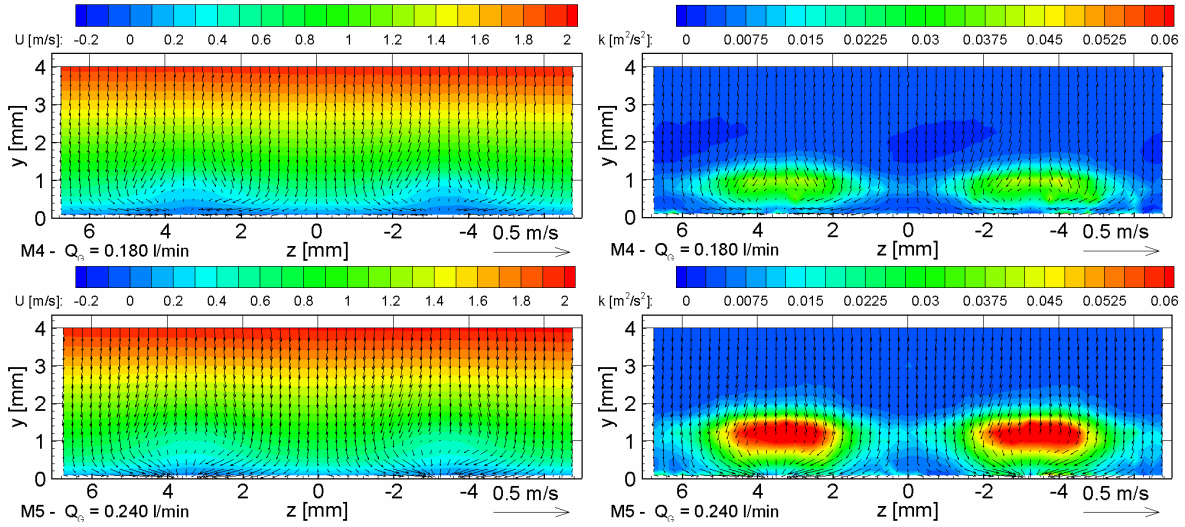

Fig.1: Velocity and turbulent kinetic energy distribution at a plane (1D) behind the suction holes

1. INTRODUCTION

The aircraft industry has always been interested in reducing the aerodynamic drag, hoping to achieve enhanced fuel economy, range and flight performance and/or reduce weight, noise and emissions. In the pursuit of less drag, an important area of research has been in aircraft wing design. Fluid flow along a flat surface is usually laminar near the leading edge. As the flow progresses downstream, factors such as surface roughness, boundary layer instabilities (e.g., Tollmien-Schlichting waves, Taylor-Goertler vortices, Rayleigh instabilities, and cross-flow disturbances), and pressure gradients may cause the boundary layer to change from laminar to turbulent. Turbulent skin friction drag can be as much as 10 times that of laminar skin friction drag for the same Reynolds number (due to the much higher wall shear stresses of turbulent flows). Thus, preventing the transition process can result in much reduced drag for the aircraft. However, although the laminar and turbulent flow conditions are well understood, the transition process that leads from one to the other is not.

Engineering attempts to maintain the laminar state at either Reynolds numbers or downstream distances beyond that which is normally turbulent or transitional is called Laminar Flow Control (LFC). In most cases, LFC entails sucking a portion of the boundary layer flow through the wall. Linear stability theory shows that continuous suction can stabilize the boundary layer and substantially increase the critical Reynolds number at which transition begins. This stabilization is accomplished by decreasing the boundary layer thickness, thereby decreasing the effective boundary layer Reynolds number. Unfortunately, continuous wall suction is unpractical from a fabrication viewpoint, and suction is usually implemented via discrete holes or sometimes slots in the wall surface. Discrete holes can lead to hole-to-hole interactions, trailing vortices, and additional suction parameters / variables.

The aim of the present work is to understand the critical parameters affecting boundary layer stabilization via suction through discrete holes. In the literature differences exist in the experimental results (Goldsmith [1957] and MacManus et. al. [1996] and Magnus, Eaton [2000]) and in DNS (Meitz [1996] and Messing, Kloker [1998]). In particular, this experimental study intends to concentrate upon resolving the differences in the two simulation studies (since they consider identical flow parameters). The figure 2 shows in a simulation of Messing and Kloker [1998] the distribution of the vorticity distribution behind a suction hole. At the height-lines of the vorticity, the mutually rotating longitudinal-vortexes whirls are recognizable. The viewed relevant current-area (integration-area) stretches on a relatively short section of approximately 5D (D - diameter of suction holes) behind the suction holes. Unknown details of the flow-structure for example: reciprocal influence of the suction holes, local effects of the intently high suction flow rate on the receptivity of the boundary layer flow, mechanisms of the self-induced transition by critical suction flow rate. Present work focused on the calculation of the suction flow configurations in three-dimensional boundary layer.

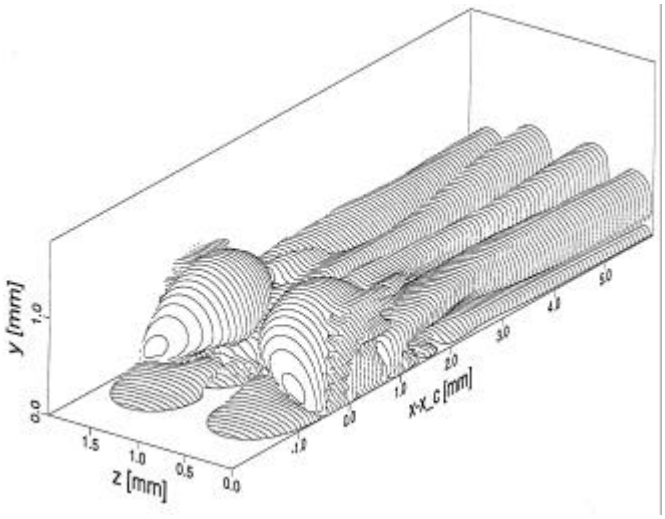

Fig. 2: DNS simulation of the vorticity distribution behind the suction holes by Messing and Kloker [1998]

2. EXPERIMENTAL METHOD and PROCEDURES

2.1 Matched Index Refraction tunnel

Quantification of boundary layer transitional flows requires measurements very close to the wall for accurate determination of the wall shear stress. LDA measurements usually suffer from optical interference or blockage of the laser beams, especially when systems for two and three component measurements are employed. Some examples of near wall flow experimental studies in fully developed pipe flows include Durst et al. [1993], Lekakis et al. [1994], and Durst et al. [1996]. Similar measurements in fully developed channel flows were conducted by Djenidi and Antonia [1993] and Durst et al. [1998].

LSTM intends to utilize several methods to improve this situation. LDA (non-intrusive) will be employed in a matched index-of-refraction (MIR) facility (no optical distortion) of very large size (higher spatial measurement resolution) to study suction LFC. Until recently, however, no refractive index matched flow facility existed that permitted reasonably-sized flat plat boundary layers to be set up and, hence this provides the basic test facility to study in detail LFC the laminar to turbulent boundary layer transition control. Figure 1 is a sketch of a MIR facility recently installed at the LSTM.

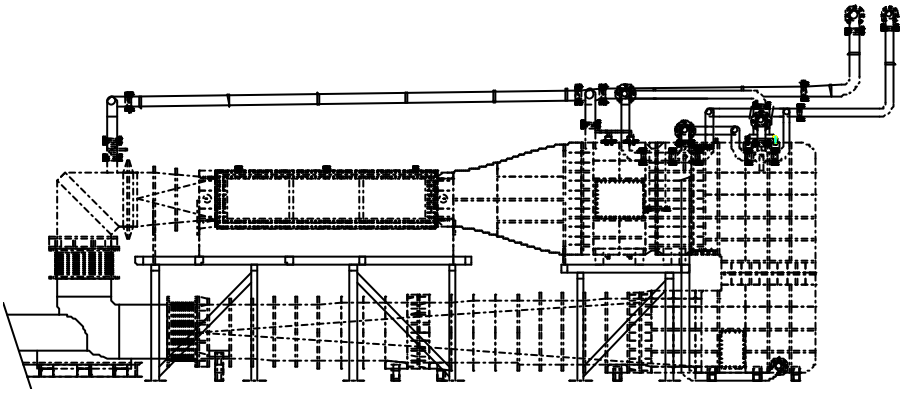

Fig.3: Matched Index Refraction tunnel at LSTM Erlangen

The big refraction index canal is a new test facility at LSTM (fig. 1). The entire installation was completed only in the last years and brought in service. An idea of the test rig with first experimental results is given in Becker [2001]. Table 1 gives a short overview of the most important technical data. As comparison, the technical parameters of a similar canal were drawn near at the INEEL in the USA. Both canals are one of a kind in this size in the world. The cross area of the test section of the LSTM canal is somewhat smaller with approximately same length of the test section, but at LSTM, can have 2.5 times higher velocity in contrast and also higher Reynolds number are reached with it. A clear difference appeared in the turbulence intensity in the test section. A turbulence intensity of approximately 0.15% was achieved at LSTM. The measurements took place with the hot-film-anemometer. And as small as possible turbulence intensity is regarded as an important condition for controlled investigations in the laminar - turbulent boundary layer transition flow.

	INEEL	LSTM
Cross area of test section	0.62 x 0.62m	0.6 x 0.45m
Length of test section	2.4m	2.52m
Contraction ratio	4:1	6:1
Fluid / oil	Drakeoel 5 (PENRECO)	Odina 913 (SHELL)
Refraction index	1.4585	1.4585
Kinematic viscosity	12.1e-6 m^2/s	11.2e-6 m^2/s
Temperature control	extern	intern
Maximum of velocity	1.9m/s	5m/s
Turbulence intensity	0.5%	0.15%

Tab. 1: Technical specifications of the Matched Index Refraction channel

2.2 Test rig

The already mentioned direct numerical simulations by Messing [1999] and Meitz [1996] formed the basis of the chosen experimental parameters. Comparison-calculations in a Blasius boundary layer yielded here, as already mentioned, deviations in the calculated current-structure that could not yet be clarified until now completely. The calculations were enforced with a defined disturbance source before the suction holes and consequently the suction influences the propagation of that itself training Tollmien-Schlichting-waves. For the experimental investigations, one gave up this defined stimulation in order to simulate the real physical transition processes behind the suction holes with "free transition" condition. Under "free transition" it is to be understood here that there are no artificially defined disturbances introduced before the suction holes in the boundary layer. The transition process in the flat boundary layer is described by the natural defined spectrum of the test facility consequently. The low turbulence-degree of the used test section proves favourably on this occasion (sees table 1). The design and location of the suction holes, the suction flow rates and the velocity around the holes are calculated on the basis of the Reynolds number and the ratio of the velocity around the suction to the outside-current velocity as in the DNS.

The drawing in figure 3 shows a complete representation of the entire test plate including the suction device. The suction is realized over a plenum, which is below the plate at the position of the hole-array. The size of the plenum is calculated empirically and is chosen from literature, so that an even velocity distribution can be guaranteed in the single suction hole. Preliminary measurements confirmed this assumption. The return of the oil into the canal takes place after the pump-unit at the end of the test section. The regulation of the suction flow rate is steered over the speed of the used pump by means of frequency controller unit. To monitor the volume suction a turbine flow rate meter with integrated electronic impulse-giver is used before the pump.

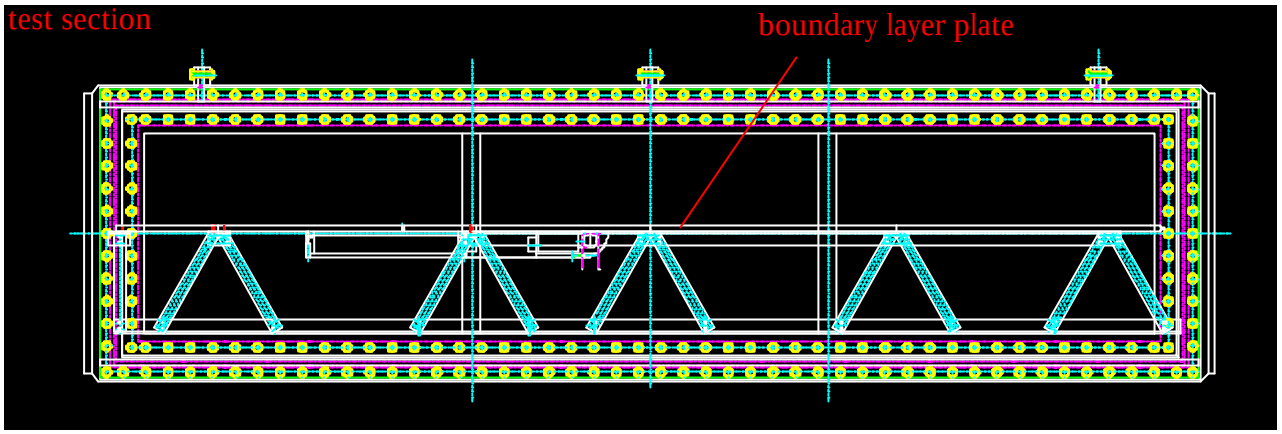

Fig. 4: Drawing of the measuring plate and the test section

Fig. 5: Test section with suction unit

The row of the suction hole consists of 43 holes with a diameter of 3.5 mm and a hole-spacing of 6.74 mm. Consequently, the row of suction holes includes 48% of the total-width of the test plate. The picture in figure 5 gives an impression of the entire attempt-installation and the suction unit once again. It shows the measuring plate in the test section with the plenum below the plate and the part of the suction control system in the canal.

2.3 Measurement Techniques

The velocity measurements take place as already described in the beginning of the chapter, using LDA (Lasers Doppler Anemometer). For the experiments, a LDA system is used on the basis of glass fibre cables (etc Lienhart [1994], Becker [1996],). The completely system can be equipped with a 2D or/and a 1D LDA probe. For the present experiments a 1D system was used, so all the three velocity field components were not measured simultaneously. The processing of the measuring signals takes place over a Burst Spectrum Analyser (BSA) and corresponding software of the company DANTEC. The figure 6 gives a schematic overview over the measuring setup.

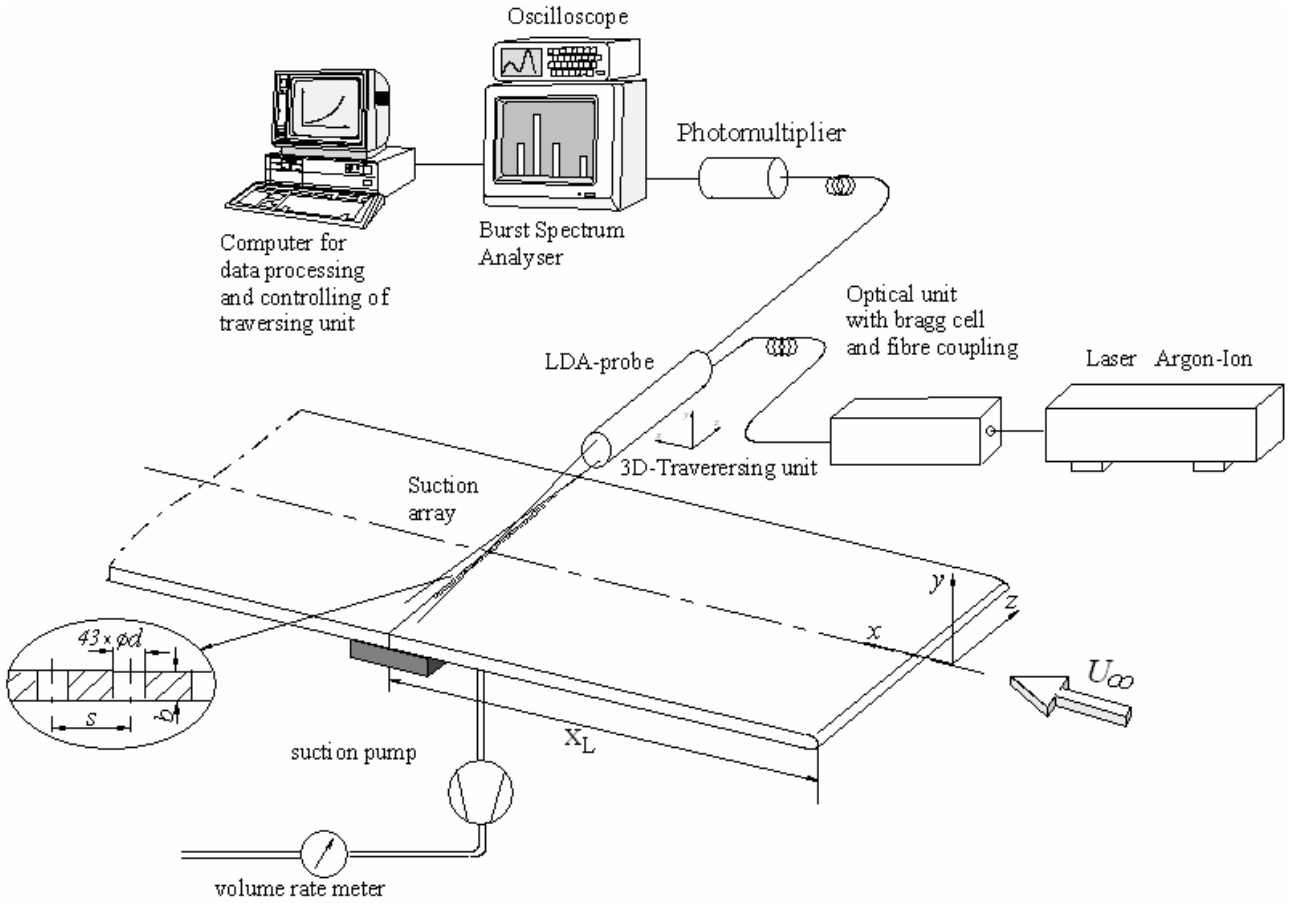

Fig. 6: Experimental setup.

3. RESULTS AND DISCUSSION

3.1 Blasius boundary layer flow

With the chosen test set up, velocity circumstances could be achieved on the upper side of the test plate so that the criterions of a Blasius boundary layer after Saric [1989] are fulfilled. The figure 7 documents the velocity profiles of the boundary layer in the middle of the plate over the plate length x. From x = 2000 mm (300mm behind the suction holes) the velocity distribution changes, that is a sign for the starting of transition. The velocity profile at the end of the plate was turbulent. The results were confirmed by the results of the rms - distribution of the velocity fluctuations (also seen in figure 7).

Beside the mean velocity and turbulence intensity distributions, holding back of the shape factor is regarded H_{12} as a crucial evaluation-criterion (see Saric [1989]). The figure 8 shows the course of the shape factor H_{12}, the displacement thickness δ_1 and the Reynolds number covered on the displacement thickness. The results document that until now met statements can be confirmed. The deviations of the form shape parameter lay in the area from smaller ± 7% up to the beginning of the transition process. The experimental conditions achieved fulfill the requirements of a Blasius boundary layer flow as presented by Saric [1989] until the area of the suction holes and also in the relevant area after it. From the simulations it emerges that the current-process relevant for the suction behavior and with it the transition process on a narrow area behind the suction holes is restricted. The natural transition process at the end the boundary layer plate has no influence on the planned investigations consequently.

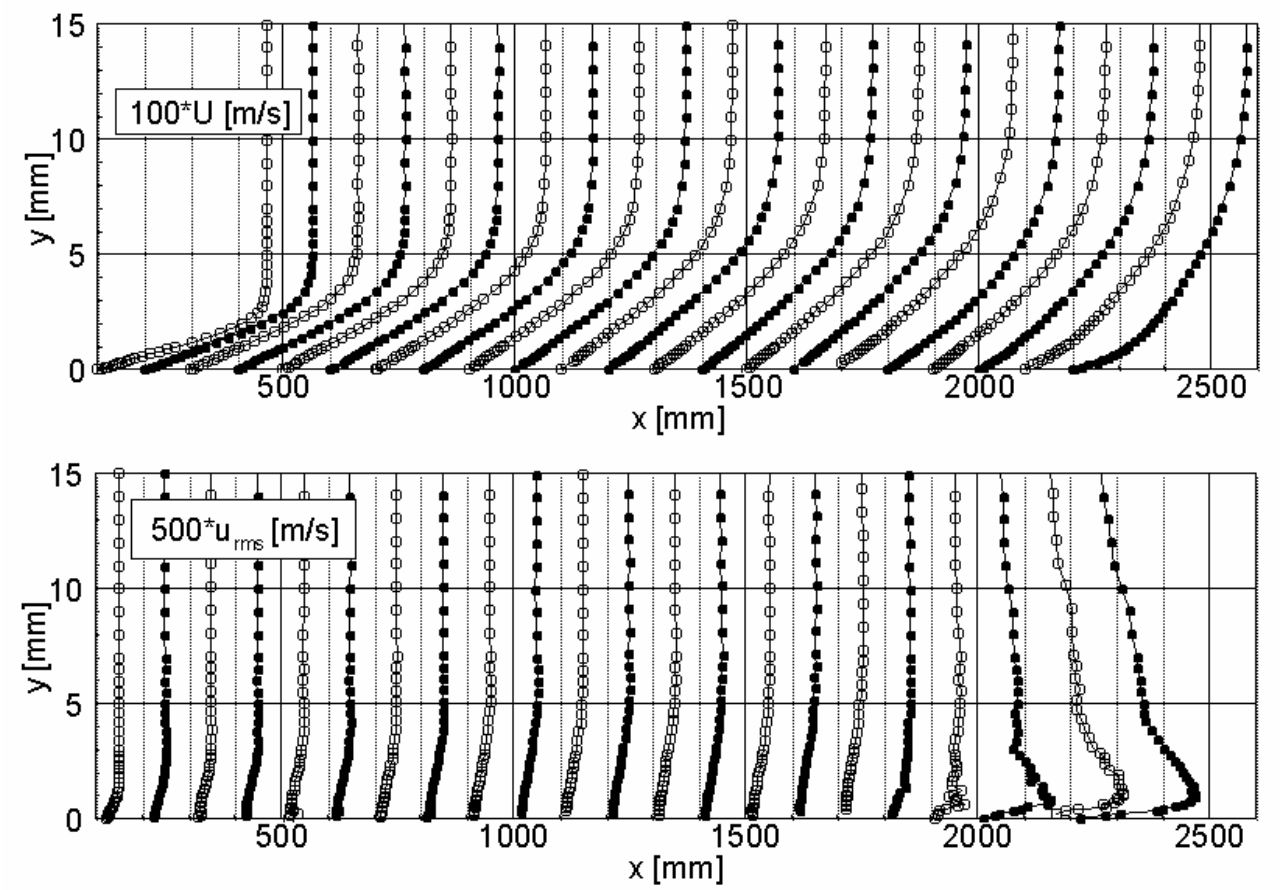

Fig. 7: Mean and rms values of the velocity profiles in boundary layer without suction

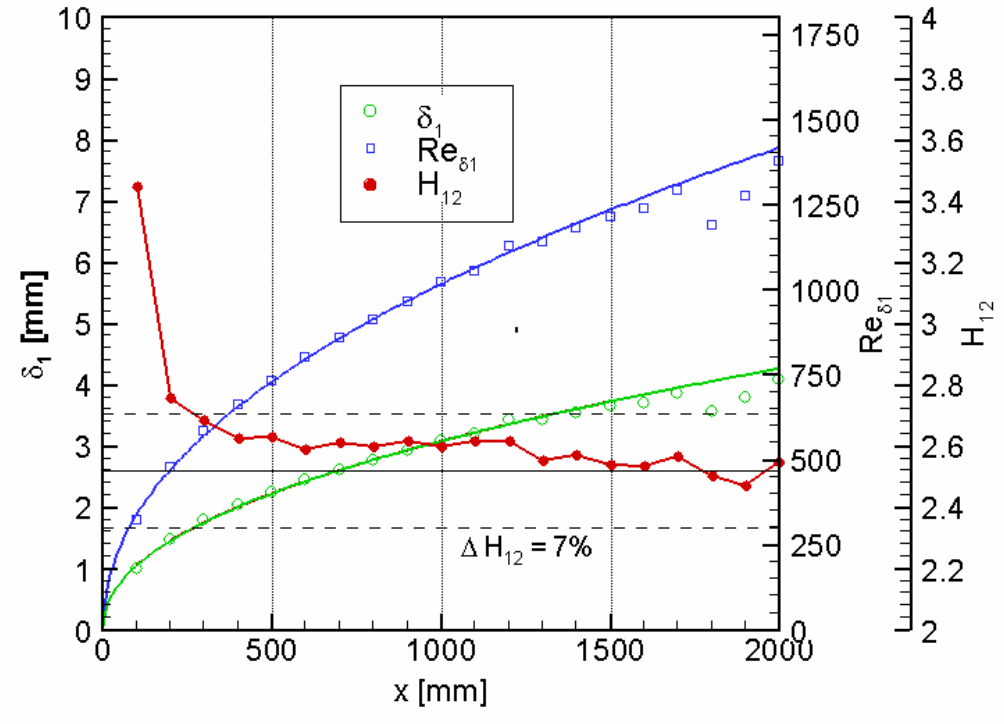

Fig. 8. Distribution of the displacement thicknessd_1, the Reynolds number Re and the shape factor H_{12} over plate length x

3.1 Parameters of the suction flow

The table 2 summarizes all measured parameters once again. The parameters of the simulation are presented by Messing [1999], the results of the calculation with the experimental test preparation and the actually achieved results from the flat plate measurements. On the basis of the small acceleration of the boundary layer and the somewhat deviant viscosity of the real fluid in the test section emerged in the experiment from the simulation and from the advance-calculation of the test construction deviant parameters negligibly. In respect to the simulations it was decided, that the experimental test parameters were in agreement with the Reynolds number based on the displacement thickness at the position of the hole-row. This meant for the investigations that a velocity, that lay negligibly higher than in the beforehand-calculations, was used intended. The Reynolds number covered on the place of the suction area lay consequently also higher than in the simulations and in the beforehand-calculations.

	Simulation	Calculation	Experiment
ν (viscosity)	1.50E-05	1.20E-05	1.12E-05
U_∞ (free stream velocity)	15 m/s	3.574 m/s	3.74m
δ_1 (displacement thickness)	1.22 mm	4.11 mm	3.67 mm
$Re_{\delta 1}$	1224	1224	1224
X_L (position of suction holes)	506 mm	1700 mm	1700 mm
Re_{x_L}	5.059E+05	5.063E+05	5.670E+05

Tab. 2: Parameter of the simulation and the experiment

Decisively with the evaluation of the results from the transition experiments is the exact knowledge of the basic flow condition in the test area. Already relatively small deviations of the pressure gradient *dp/dx* of the value zero can have a relatively strong influence on the stability qualities and the propagation of disturbances. For an estimation of the boundary layer behavior of the realized flat plate boundary layer against small disturbances, the stability-diagram from the University of Stuttgart (Messing [2001]) was used for the concrete test case conditions. The measured velocity distribution U(x) outside of the boundary layer formed the basis for the calculation of the stationary two-dimensional basic flow. The procedure is based on the numerical solution of the incompressible Navier-Stokes-equations. (see etc Fasel [1974], Rist [1990], Kloker [1993])

The figure 9 shows the measured values of the displacement thickness and the results of the calculations. Up to the row of suction holes and in the immediate area behind it, very good agreement of the results with the experiments could be achieved. It needs to be mentioned that the calculated shape factor H_{12} is essentially more sensitive to accelerations and decelerations in the outside flow as that in the experiment observed.

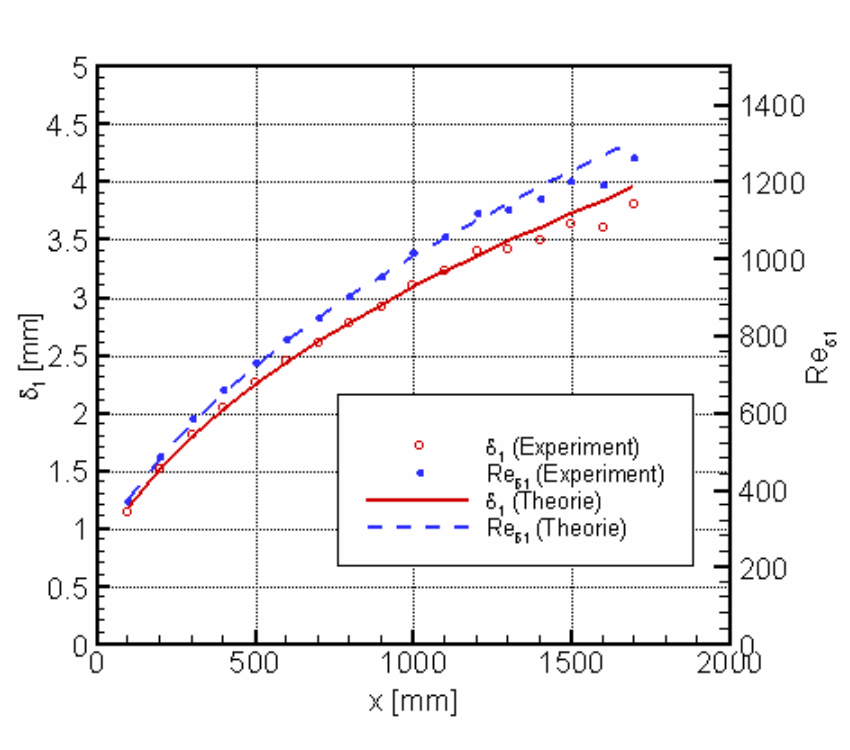

Fig. 9: Shape factor in the plate boundary layer without suction

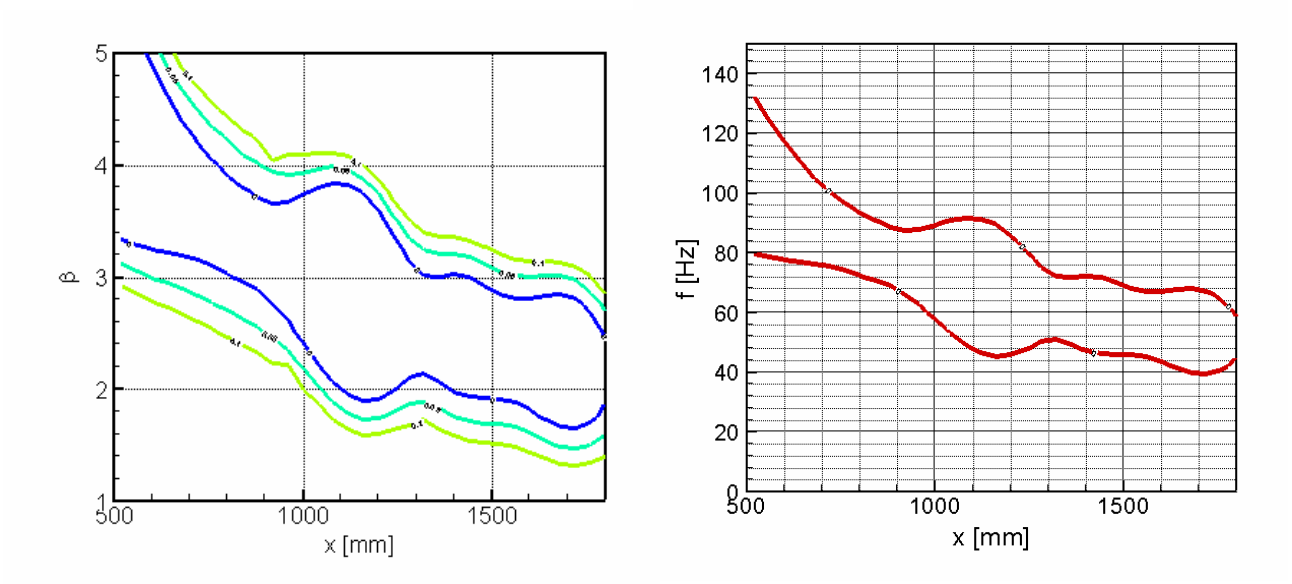

Fig. 10: Stability diagram: a) contour plots of the amplified perturbation rates b) the neutral instability-frequencies f calculated from it

From the diagram, instability-frequencies result, those in the range of 40 - 70 Hz are localized. These statements agree with the results in Schlichting [2000] for the same Reynolds number.

Flow conditions are another important point for the direct comparison of the simulations to the experiments at the suction hole directly. The direct numerical simulation by Messing, Kloker [1998] and Meitz [1996] used a $\cos^3$ -velocity distribution relation over the suction hole. This and other suitable assumptions were chosen on the basis of stability criterion for the simulations. The experimental measurements yielded that the assumption is not durable for the experiments. In good approximation, one can go out here of a block-profile at the entrance into the suction holes area. In

figure 11, the relation to this velocity distribution is represented over a single suction hole. For this situation the velocity was non-dimensionalised based on the average velocity over the suction hole. In figure 11 the $\cos^3$ curve of the simulation is also included. Both curves present the same volume rate of suction. It depicts completely different velocity distributions on the entrance of the hole (comment: the presented profile is rotation-symmetric, so that the outside-areas have an essentially stronger weighting in the calculation of the volume rate). Important for further investigation is the influence of the velocity profile on the value of the critical suction flow rate, which would be clarified here.

In the simulations as reference parameter the maximum speed in hole centre in the relationship to the outside free stream velocity is used to characterize different situations for sub critical, critical and overcritical suction rate. So for example, the critical case of the suction rate was analyzed by a relationship of about 0,55-0.6 (maximum velocity in the hole to free stream velocity). This parameter could not be drawn near the experimental investigations on the basis of the present results. It appears more meaningful to use the velocity relationship on an average velocity over the suction hole, which means a corresponding volume rate. Interestingly for the future work, here would be a repetition of the DNS deal with same test parameters.

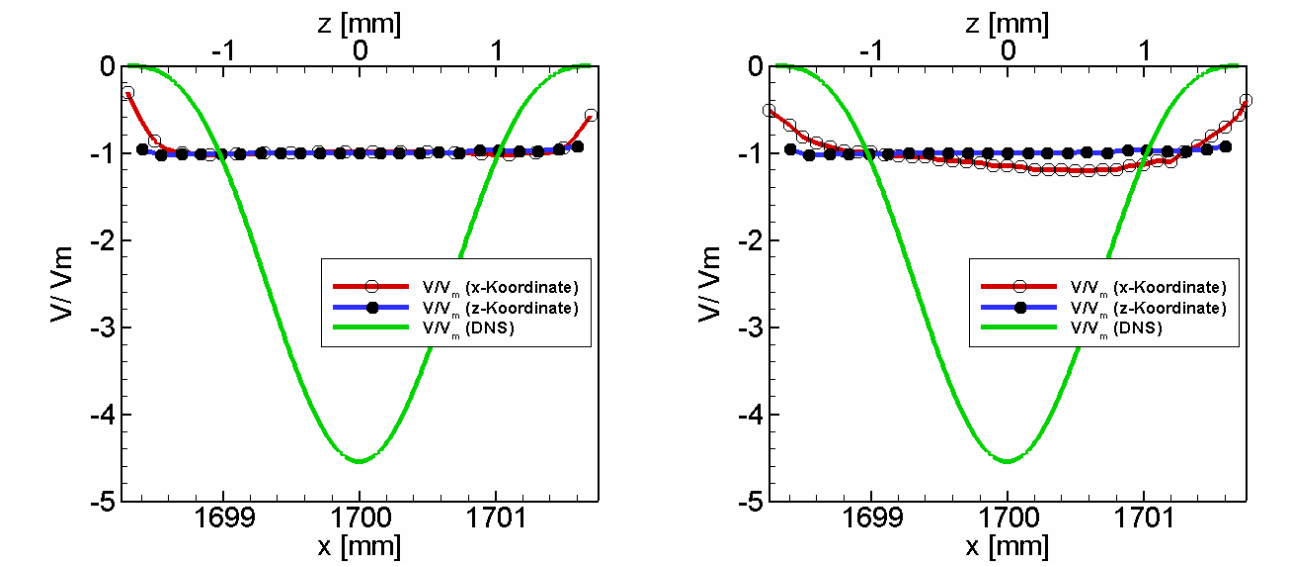

Fig. 11: Comparison between experiment and simulation of the velocity distribution over the suction holes a) without oncoming flow b) with oncoming flow

		M1	M2	M3	M4	M5	M6
V_C/ U_∞ (DNS)		0	0.4	0.5	0.6	0.8	1.0
V_M/ U_∞ (Exp)		0	0.087	0.109	0.131	0.175	0.218
Q_G	l/s	0	0.120	0.150	0.180	0.240	0.300
Q_L	mm^3/s	0	2790	3488	4186	5581	6976
Re_M		0	90.6	113.3	135.9	181.3	226.6
V_M	m/s	0	0.29	0.36	0.44	0.58	0.73

Tab. 3: Test parameter by different suction flow rate Q

The table 3 summarizes the selected test parameter in an overview with the investigations with suction. The parameters were chosen so that the area of the sub critical, critical and overcritical suction is covered with it.

3.3 Velocity and turbulence intensities in the suction boundary layer flow

The previous measurements took place in the level behind the centre of the hole. In figure 12 and 13, the velocity profiles and the turbulence intensity distributions are represented for a sub critical and overcritical suction flow rate in the comparison to the profiles without suction.

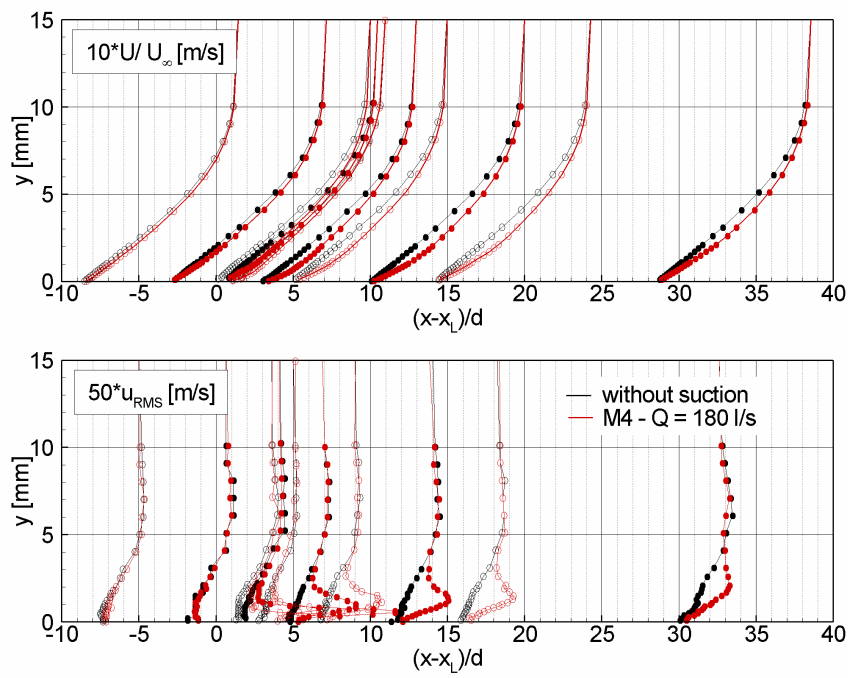

Fig. 12: Velocity and turbulence intensity profiles for sub critical suction flow rate

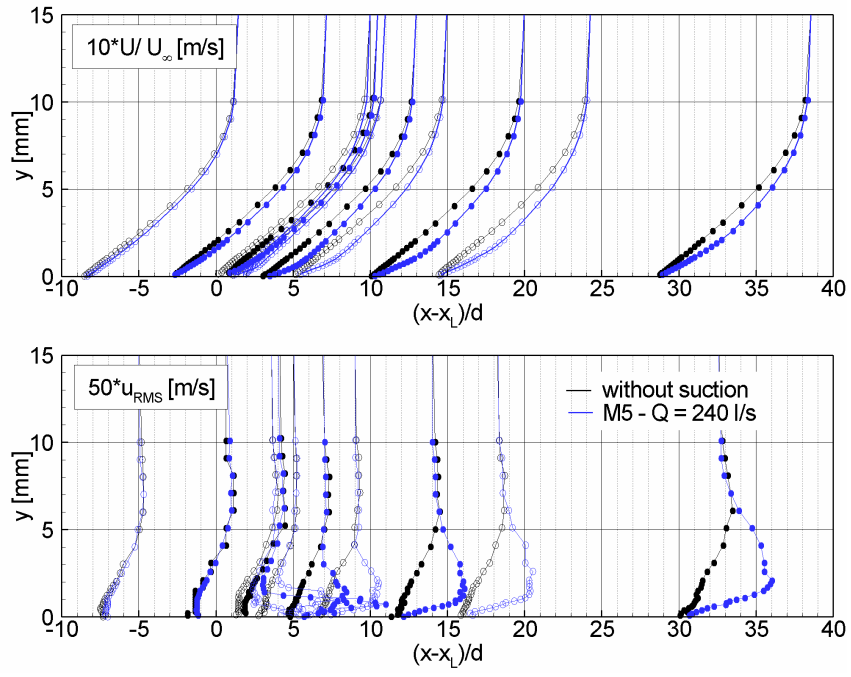

Fig. 13: Velocity and turbulence intensity profiles for overcritical suction flow rate

The figures 12 and 13 cover that a disturbance peak develops behind the suction holes in the boundary layer that outside stream up, from the wall away, hikes. For the sub critical test case, this peak is damped out, amplification occurs with overcritical suction flow rate and with it to an acceleration of the transition process.

This characteristic behavior of the disturbance peak is also to be found with it in the v-component, like the figure 14 on the basis of the velocity measurements plainly shows.

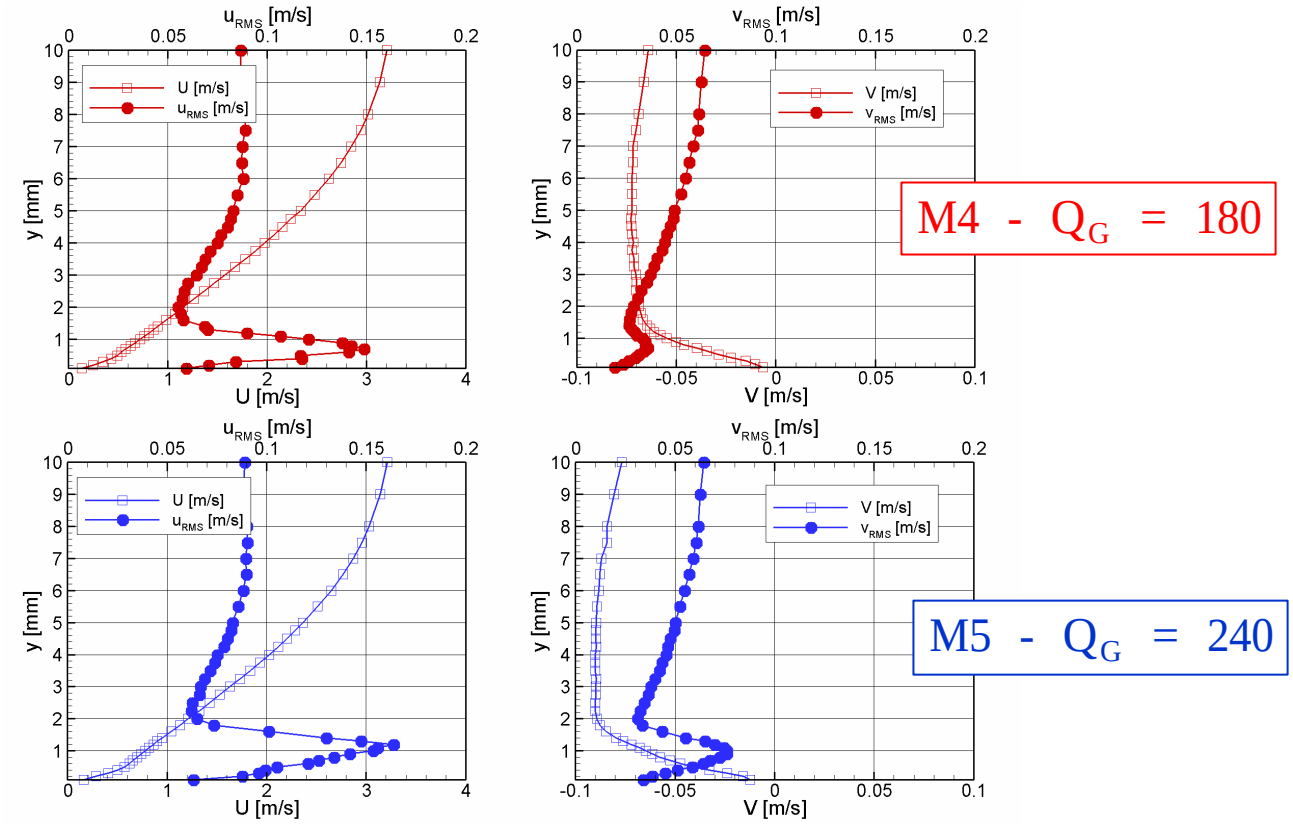

Fig. 14: Boundary layer velocity profiles and turbulence intensity distributions with a) sub critical and b) overcritical suction flow rates with 1D (hole-diameters) behind the suction hole

To have a better understanding of the physical processes of the boundary layer transition it is important to get more information about the time dependent behavior of the flow. For this purpose the power density spectrum based on velocity time signal was processed. The spectrum was calculated at the position of the maximum turbulence intensity in the boundary layer. The data rate amounted to 100 Hz approximately with a measuring time of about 200s as well as 600s (sees figures 15).

The calculation of the power density spectrum of the velocity necessitated that in not equal time steps arriving burst signals are transferred into a constant time-screen (Sample & Hold method). The maximum at most resolvable frequency of the Fourier analyses emerges in accordance with the Nyquist-Criteria to:

$$f_{max} = \frac{1}{2\,\Delta t}$$

The parameter marks the constant time-interval, in which the measuring data are processed. For the calculation of the spectrum the equation by DANTEC [2000] and Becker et al. [1996] was used:

$$S(f) = \frac{\Delta t}{N}\left|\sum_{n=0}^{N-1} x_n e^{-i\,2\Pi f n \Delta t}\right|^2$$

The so calculated power density spectrum in figure 16 shows no dominant frequencies for both test cases. On the basis of the data rate, the still resolvable frequencies lay in the area of 50Hz however and consequently in the low area of the Tollmien-Schlichting-instabilty . But nevertheless the results point toward figure 16 in context with figure 14 as a result, that the transition process is not introduced over a Tollmien-Schlichting-instability but must be understood as a stochastic process.

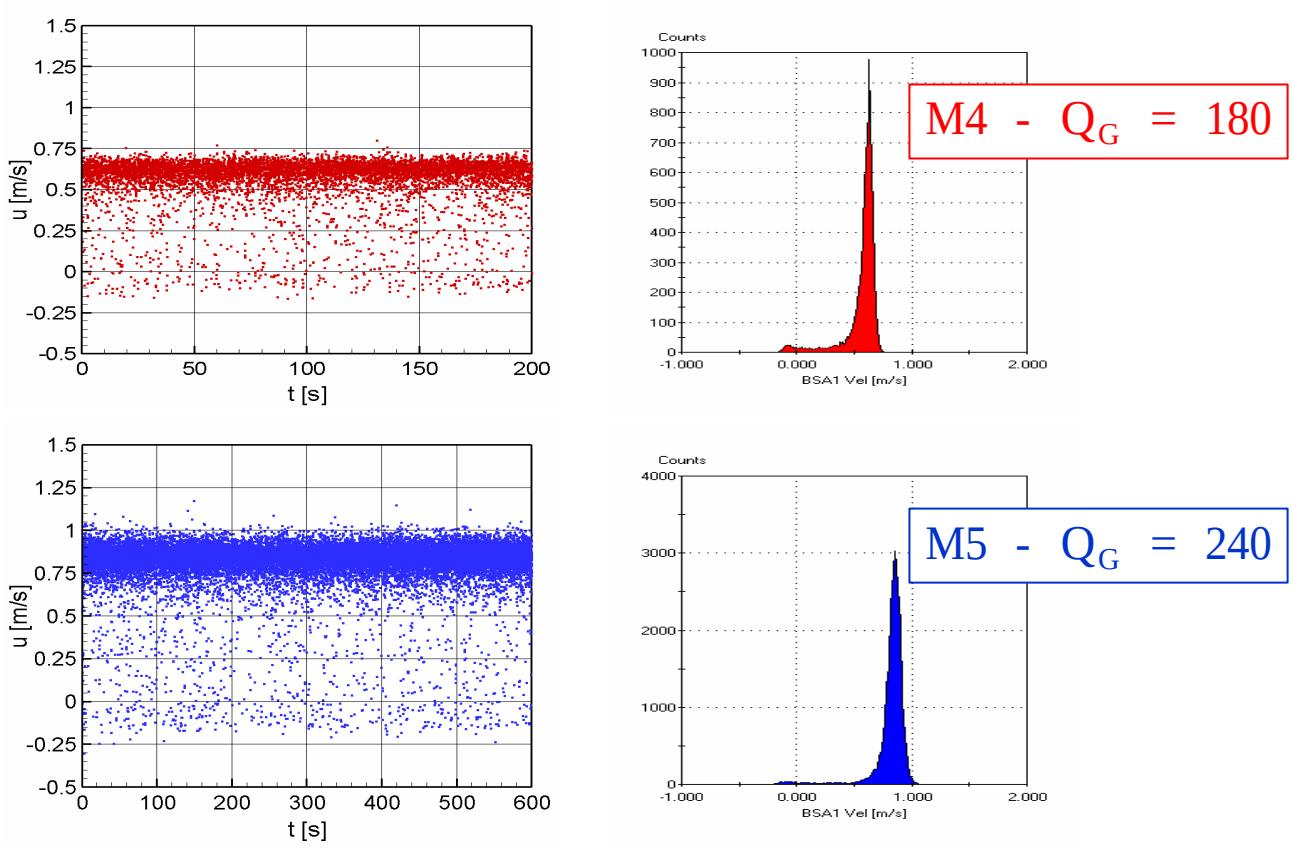

Fig. 15: Velocity-time course for a) sub critical and b) overcritical suction flow rate

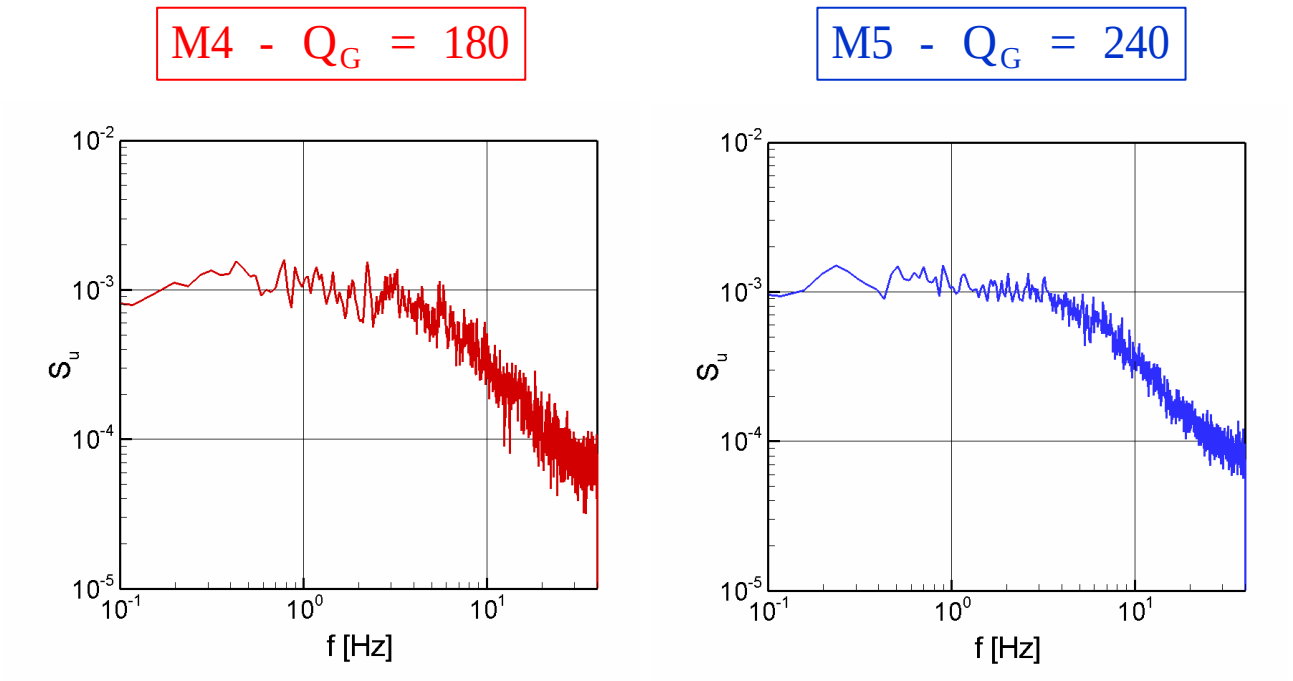

Fig. 16: Power density spectrum for a) sub critical and b) overcritical suction flow rate

3.4 Turbulent kinetic energy distribution behind the suction holes

The figure 17 shows the three-dimensional velocity-field and distribution of the turbulent kinetic energy in a plane section 1D behind the suction holes for sub critical and overcritical suction flow rates. The centre of the suction hole is located by x = 0. It is clear recognizable the strong interaction of the neighboring suction holes, their influence increases itself with the increase of the suction rate strongly, in the results. The velocity field has three-dimensional structures. In contrast to the DNS simulations, a recirculation zone could not be observed between the holes.

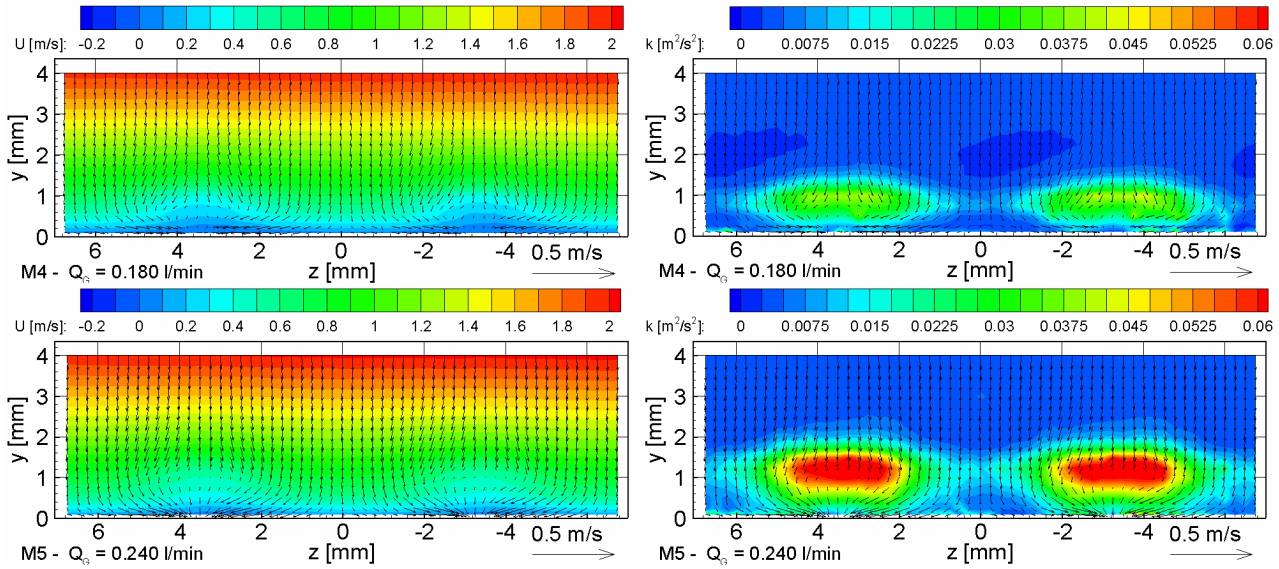

Fig. 17: Velocity field und turbulent kinetic energy distribution

4. SUMMARY

In the paper presented the experimental results in comparison to the DNS simulations. It shows that the transition process behind the suction holes is different from what it is known from the classical linear stability theory. Behind the suction holes the turbulence intensity profiles show a disturbance peak, which is in the case for the sub critical flow rate damped out further downstream. For the supercritical suction rate the peak is increasing in flow direction and causes the transition process of the boundary layer flow. Additional FFT analysis of the velocity - time series leads to the result, that the transition process is not dominated by a specific instability frequency. The transition from laminar to turbulent tends to be a stochastic process and seems to be better described by using the invariant theory.

5. ACKNOWLEDGEMENTS

The present works were promoted by the German research foundation (DFG) under the reference BE 2129/4. Additional we are thankful to the chair of the institute F. Durst and the co-workers of the institute H. Lienhart and J. Jovanovic for their steady support and valuable discussions. Useful discussion during completion of the manuscript with I. Ali is also gratefully acknowledged.

REFERENCES

Batia [1982] Bathia, Durst, F. and Jovanovic, J., Correction of hotwire anemometer measurements near walls, Journal of Fluid Mechanics, Vol. 122, pp. 411 – 431, 1982

Becker et al. [2000] Becker, S, Lienhart, H., Durst, F.: Flow around three dimensional obstacles in boundary layers, Journal of Wind Engineering and Industrial Aerodynamics, 90(4-5), pp. 265-279, Elesevier, (2002)

Becker et al. [2001] Becker, S., Stoots, C., Lienhart, H., McEligot, D., Durst, F,: Refractive Index Matched LDA Technique for Investigations of Laminar to Turbulent Boundary Layer Transition, 2nd International Symposium on Turbulence and Shear Flow Phenomena, Stockholm, (2001)

Becker [2002] Becker, S., Stoots, C.M., Condie, K., Durst, F. and McEligot, D., LDA Measurements of Transitional Flows Induced by a Square Rib, J. of Fluid Engineering, Vol. 124, 2002

DANTEC [2000] Handbook BURSTware, 2000

Djenidi and Antonia [1993]: Djenidi, L.; Antonia, R. A.: "LDA measurements in low Reynolds number turbulent boundary layer," Experiments in Fluids, Vol. 14, pp. 280-288, 1993.

Durst et al. [1993] Durst, F.; Jovanovic, J.; Sender, J.: "Detail Measurements of the Near Wall Region of Turbulent Pipe Flow," FED-Vol. 146, Data for Validation of CFD Codes, ASME, Book No. H00786, pp. 79-86, 1993.

Durst et al. [1995] Durst, F., Jovanovic, J. and Sender, J., LDA measurements in the near wall region of a turbulent pipe flow, Journal of Fluid Mechanics, Vol. 295, pp. 305 – 335, 1995

Durst et al. [1996] Durst, F.; Kikura, H.; Lekakis, I.; Jovanovic, J.; Ye, Q.: "Wall shear stress determination from near-wall velocity data in turbulent pipe and channel flows," Experiments in Fluids, Vol. 20, pp. 417-428, 1996.

Durst et al. [1998] Durst, F.; Fischer, M.; Jovanovic, J.; Kikura, H.: "Methods to set up and investigate low Reynolds number, fully developed turbulent plane channel flows," Journal of Fluids Engineering, Vol. 129, pp. 496-503, 1998.

Fasel [1974] Untersuchung des Grenzschichtumschlages durch numerische Integration der Navier-Stokes Gleichungen, Dissertation, Universität Stuttgart, 1974

Goldsmith [1957] Goldsmith, J.: "Critical Laminar Suction Parameters for Suction into an Isolated Hole or a Single Row of Holes," NAI-57-529 (BLC-95), Northrop Aircraft Inc., 1957.

Kloker [1993] Direkte Numerische Simulation des laminar-turbulenten Grenzschichtumschlages in einer stark verzögerten Grenzschicht, Dissertation, Universität Stuttgart, 1993

Lekakis et al. [1994] Lekakis, I.; Durst, F.; Sender, J.: "LDA Measurements In the Near Wall Region of an Axis symmetric Sudden Expansion," Proceedings of 7th International Symposium on Applications of Laser Techniques to Fluid Mechanics, Lisbon, Portugal, July 11-14, pp 13.6.1-13.6.8, 1994.

MacMagnus et al. [1996] MacManus, D. G.; Eaton, J. A.; Barrett, R. V.; Richards, J.; Swales, C.: "Mapping the Flow Field Induced by a HLFC Perforation Using a High Resolution LDV," AIAA-96-0097, 1996.

MacMagnus and Eaton [2000] McMagnus, D.G., Eaton, J.A, Flow physics of discrete boundary layer suction – measurements and predictions, J. Fluid Mech., vol.417, pp 47-75, 2000

Meitz [1996] Meitz, H.L., Numerical investigations of suction in a transitional flat-plate boundary layer, Dissertation, Department of Aerospace and Mechanical Engineering, University of Arizona, 1996

Messing and Kloker [1998] DNS-Untersuchung der diskreten Absaugung durch Einzelloch- Arrays, 2. Zwischenbericht zum Forschungsvorhaben 20A 9505G, Universität Stuttgart, 1998

Messing [2001] private communications and project discussions

Rist [1990] Rist, U: Numerische Untersuchung der räumlichen, dreidimensionalen Störungsentwicklung beim Grenzschichtumschlag, Dissertation, Universität Stuttgart, 1990

Saric [1986] Saric, W.S., Reed, H.L.: Effect of suction and weak mass injection on boundary layer transition, AIAA Journal, Vol.24, No3, 1986

Stoots et al. [2001] Stoots, C., Becker, S., Condie, K., Durst, F. and McEligot, D., A large-scale matched index refraction flow facility for LDA studies around complex geometries, Experiments in Fluids 30, Springer Verlag, 2001